Source and Propagation Characteristics of Kilometric Continuum Observed with Multiple Satellites

K. Hashimoto
RISH, Kyoto University

R. R. Anderson
University of Iowa

J. L. Green
NASA/GSFC

H. Matsumoto
RISH, Kyoto University

Short title: KILOMETRIC CONTINUUM

Abstract.

Kilometric continuum radiation was first identified with the GEOTAIL Plasma Wave Instrument (PWI) as the high frequency extension of escaping continuum emissions in the frequency range from 100 kHz to 800 kHz. It consists of from a few to many narrow-band emissions. It was observed mainly near the magnetic equator, and its source was expected to be inside of the plasmapause and the topside equatorial region. Recently, data from the IMAGE Radio Plasma Imager (RPI) and Extreme ultraviolet (EUV) experiments have been used to show that kilometric continuum is generated at the plasmapause, in or near the magnetic equator, within a notch region, and have confirmed the expectation. Data from the CRRES PWI have also identified other sources from the equatorial density irregularities. An example of CRRES observations reveals a possibility that kilometric continuum has been radiated as a wide beam emission. The IMAGE and GEOTAIL simultaneous observations are not like the previous observations since they show it has been observed to have a very broad emission cone. It could also be the highest frequency continuum enhancement so far observed since it is associated with a high energy electron injection event.

Introduction

Kilometric continuum radiation was first identified in the Sweep Frequency Analyzer (SFA) data of the GEOTAIL Plasma Wave Instrument (PWI) [Matsumoto et al., 1994] as the high frequency extension of escaping continuum emissions in the frequency range from 100 kHz to 800 kHz [Hashimoto et al., 1999]. It consists of from a few to many narrow-band emissions that are observed mainly near the magnetic equator. The other emissions most frequently encountered in this range are Auroral Kilometric Radiation (AKR) and Type III solar radio bursts. The kilometric continuum frequency spectra are composed of discrete components like escaping continuum, and its intensities are usually much weaker than AKR but are similar to those of escaping continuum [Kurth et al., 1981].

The source mechanism is expected to be electrostatic waves near the plasma frequency that are mode-converted into electromagnetic waves [e.g., Jones, 1976]. If the emissions detected by GEOTAIL originate at the plasma frequency, their highest frequencies must come from deep inside the plasmasphere at an altitude of less than a few thousand kilometers in the topside equatorial region of the Earth's ionosphere. These measurements therefore suggest the discovery of a new component of continuum coming from inside the Earth's plasmasphere, and also suggest that the source of these emissions ought to be detected by other satellites in that region of the magnetosphere [Hashimoto et al., 1999].

Recently the IMAGE Radio Plasma Imager (RPI) and Extreme ultraviolet (EUV) observations have indicated that kilometric continuum radiation is generated at the equatorial plasmapause within a notch region of the plasmasphere [Green et al., 2002]. Later, [Green at al., 2004] examined the relation between the notches and kilometric continuum and concluded that 'a density depletion or notch structure in the plasmasphere is typically a critical condition for the generation of kilometric continuum but that the notch structures do not always provide the conditions necessary for the

generation of the emission.'

The CRRES satellite had a quasi-equatorial orbit and observed much kilometric continuum including source regions inside the plasmapause. **Carpenter et al.** [2000] reported equatorial density structures in detail using the CRRES data. These observations identified some examples of source regions. Although **Green et al.**, [2000] stated that it is not known if the notch region is a necessary condition for the generation, the present paper shows clear evidences that sources other than the notch region also exist. An interesting spectral structure is examined to test the linear mode conversion theory [e.g., **Jones**, 1976 and 1980].

A simultaneous kilometric continuum observation by GEOTAIL and IMAGE is also examined and it indicates a wide beam emission contrary to Jone's beaming theory. The frequency range of the continuum was from 400 kHz to 750 kHz. This is identified to be enhanced continuum although one does not expect to observe it in this frequency range since all observations of the emission have been reported to be up to about 100 kHz.

Menietti et al., [2003] made multi-spacecraft observations of kilometric continuum by Polar, GEOTAIL, and Cluster and confirmed a possible mode-conversion source mechanism near a region of high density fluctuations. High-resolution kilometric continuum data by Polar and Cluster with closely spaced emission bands were shown.

Observations of kilometric continuum at 252 kHz and 500 kHz by INTERBALL-1 were given by **Kuril'chik et al.**, [2004]. They discussed the dependency of beam widths on solar activities. The **Hashimoto et al.** [1999] study found that the kilometric continuum occurrence probabilities are high only near the equator. This dependency will be re-examined as well.

CRRES Observations

CRRES was launched on July 25, 1990, into a geosynchronous transfer orbit with a perigee altitude of 350 km and an apogee of 6.3 Re (Earth radii) geocentric. The

inclination was 18.2° and the orbital period was 9 h and 55 min. The CRRES plasma wave experiment instrumentation [Anderson et al., 1992] was designed to measure the plasma wave environment in the Earth's radiation belts with emphasis on high-frequency and high-time resolution, a large dynamic range, and sufficient frequency response to cover all of the characteristic frequencies of the plasma that are of interest. The frequency range was constrained by available technology and telemetry limitations. The combination of a sweep frequency receiver (SFR) and a multi-channel analyzer (MCA) provides measurements of electric fields from 5.6 Hz to 400 kHz and magnetic fields from 5.6 Hz to 10 kHz with a dynamic range of at least 100 dB. The electric field was detected by a 100-m tip-to-tip extendable fine wire long electric dipole antenna.

Figure 1 shows the spectra of the electric field from 5.6 Hz to 400 kHz observed for 10 hours beginning at 15:35 UT on October 10, 1990. The observed UT, geocentric distance in earth radii (R), magnetic latitude (MLAT), magnetic local time (MLT), and L value (L) are shown at the bottom. The intensities are shown color coded by the scale above the plot in dBV/m/$\sqrt{\text{Hz}}$. The red line beginning above 400 kHz at perigee and extending down to below 4 kHz at apogee is the electron cyclotron frequency f_H. The three or more emission bands immediately above f_H are electron cyclotron harmonic emissions. The narrow emission line which appears at 400 kHz at about 16:10 UT and then decreases to lower frequencies is at the upper hybrid resonance frequency f_{uhr}. Since $f_{uhr} = \sqrt{(f_p^2 + f_H^2)}$, where f_p is the electron plasma frequency, $f_{uhr} \sim f_p$ when $f_p >> f_H$. The steep electron density drop seen near 1635 UT is the outbound plasmapause. Continuum emissions are observed outside of the plasmapause up to almost the highest frequencies of the receivers. The narrow-band emissions which start from about 30 kHz up to about 100 kHz are escaping continuum radiation. The emissions from about 200 kHz up to almost 400 kHz are kilometric continuum radiation. The continuum emissions are electromagnetic waves mode-converted from electrostatic waves at the steep density gradient. They are consistent with the linear conversion theory [e.g. Jones, 1976 and

1982]. Here the plasmapause is a probable source of kilometric continuum. Note that the plasmapause for this orbit lies very close to the geomagnetic equator.

Figure 2 shows the observations for two hours beginning at 23:50 UT on September 6, 1990. Electromagnetic emissions around 200 kHz are generated after the mode conversion at density perturbations inside the plasmapause at 0010 UT and are propagated outside of the plasmasphere as expected [Hashimoto et al., 1999]. Emissions from sharp gradients are also observed by Menietti et al., [2003]. Other components of the escaping continuum are also generated at lower frequencies. The observations are evidences of a source of kilometric continuum radiation other than the notches discovered by IMAGE [Green et al., 2002]. Note that the emissions again are generated close to the geomagnetic equator.

Kilometric continuum radiation was observed near the equator on August 19, 1990, as shown in Figure 3, which extends for 10 hours beginning at 21:20 UT. New interesting characteristics of the kilometric continuum are seen above 100 kHz from 2320 UT to 0320 UT while CRRES was well outside the plasmapause. The low frequency normal continuum and the higher frequency kilometric continuum could have different source regions. In fact the small break in the emission spectra around 80 kHz gives one the impression that they are coming from two distinct sources. The durations of the emissions are different for frequencies from 100 to 300 kHz. Below 300 kHz, the durations are longer at lower frequencies. If the durations were limited by a plasma wall like a notch extending in longitude, they would be longer for higher frequencies. Therefore, they could be related to the effect of the beaming. Figure 4 shows the orbit of CRRES as a pink curve in the geomagnetic coordinates Xmag and Ymag in Re. Blue lines and the labels 23:32 and 26:52 (which corresponds to 02:52 UT the following day) show the observed time limits for the 100 kHz waves. The green, yellow, and red lines and labels correspond to the observed time limits for 145, 180, and 225 kHz, respectively. This trend of the observed boundary is consistent with the beaming theory.

The source position of Xmag = 3.9 Re was determined from the plasmapause position based on detailed examination of Figure 3. Ymag (the north-south coordinate) was determined from the assumption of the symmetry between the start and end points of the observation. The angles between the lines and the equator are the beaming angles, $\alpha = \tan^{-1}(f_H/f_p)$, where f_H and f_p are the local cyclotron and plasma frequencies, respectively [**Jones**, 1980 and 1981]. Observation examples consistent with the theory are given by **Jones et al.** [1987]. Since the radiated frequencies are equal to the plasma frequencies and the cyclotron frequency is assumed to be 14.8 kHz at 3.9 Re based on the dipole model, α can be calculated as shown in Figure 5a. The green and red lines show the theoretical and observed values, respectively. At and below 225 kHz, the observed trends are quite similar and consistent with the theory, but the values are different. The 300 kHz observation in Figure 5 shows higher α and this trend is consistent if its source altitude is lower which means higher f_H. The position of the plasmapause at this frequency is inside of that at the lower frequencies. Since the source of the 300 kHz waves are expected to be further inside the plasmapause according to Figure 3 where the local f_H is higher, its theoretical α is expected to be larger. If the source Xmag were 4.3 Re, the theory and observation results would be closer as shown in Figure 5b. However, this would not be possible according to Figure 3. If we had not had such data, we could have concluded the existence of a remote source. Another problem is that the kilometric continuum radiation is continuously observed even over the equator contrary to the theory. These results for our kilometric continuum radiation observations are consistent with the objections to the theory raised by a study of terrestrial continuum radiation [**Morgan and Gurnett**, 1991].

IMAGE and GEOTAIL Observations

The IMAGE spacecraft was launched on March 25, 2000 into a highly elliptical polar orbit with initial geocentric apogee of 8.22 RE and perigee altitude of 1000 km. The

Radio Plasma Imager (RPI) instrument on IMAGE is a highly flexible radio sounder that transmits and receives coded radio frequency pulses in the frequency range from 3 kHz to 3 MHz [Reinish, et al., 2000]. RPI also makes passive radio measurements. RPI utilizes three orthogonal dipole antennas of 325 m (X axis), 500 m (Y axis), and 20 m (Z axis). The X axis antenna was originally extended to 500 m but was shortened to 325 m when it apparently collided with space debris on October 3, 2000. The RPI instrument alternates between making passive radio wave measurements and radio sounding measurements. Each of these modes of operation is analyzed and displayed differently.

The passive radio wave observations of kilometric continuum with IMAGE RPI are displayed in a frequency-versus-time spectrogram with a frequency range of 300 – 800 kHz in the top of Figure 6. The simultaneous observation by GEOTAIL PWI is shown in the bottom of Figure 6. The three-hour Kp values were 4, 4-, 4-, 3, 7, 8-, 8+, 8, and 7+, 5+, 4, 3, 4-, 6, 5, 6 on May 29 and 30, respectively. The kilometric continuum was received during the disturbed time, especially Kp > 7 from 20 UT to 03 UT. The kilometric continuum with quite good similarity can be seen from 21 UT to 06 UT in both spectra including the fine structures. IMAGE moved from the southern hemisphere to 30°N. On the other hand, GEOTAIL moved from 4.4°N to 12.3°N at 01 UT, then 2.4°N as shown in the right of Fig. 6. Both satellites observed almost the same spectra in a wide latitude range of more than 30°. Their longitudes are close within 10°. These observations are very uncharacteristic of kilometric continuum reported by [Hashimoto et al., 1999] and [Green et al., 2002] due to the wide latitudinal spread of the emission observed by IMAGE RPI. The vertical line at 0420 UT is a type III burst. The intensity observed by IMAGE is weaker around 400 kHz after 0430 UT where the satellite is in latitudes higher than 25°. It would be difficult to explain these quite similar spectra by multiple narrow beam sources. This can be rather explained if the sources radiate in wide directions in latitude and both satellites receive the emissions from the same or

close sources contrary to the beaming theory.

These observations are during a time when the LANL geosynchronous spacecraft observed injections of high-energy elections which is an observed characteristic of continuum enhancement [see: **Gough**, 1982; and **Kasaba**, et al., 1998]. These observations may be the highest frequency continuum enhancement emissions observed although no broadening of the discrete bands are seen. It is important to note that these emissions are observed on the nightside, outside the plasmasphere over the same frequency range of AKR but since there is no observed AKR we are able to measure these emissions. This may be the reason why continuum enhancements have not been found in the this frequency range before.

The kilometric continuum frequency range has been stated as being from about 100 kHz to 800 kHz because it has been observed over the entire range of frequencies covered by the upper band of the GEOTAIL SFA. Many examples of the kilometric continuum being an extension of escaping continuum radiation beginning well below 100 kHz have also been observed. The actual frequencies could be higher and above the PWI upper cutoff frequency. The highest frequency kilometric continuum IMAGE ever observed is, however, 800 kHz. Although the frequency range of the IMAGE RPI goes to 3 MHz, the spectrogram data is routinely taken up to 1 MHz.

Discussion and Conclusions

Since **Kuril'chik et al.**, [2004] reported the dependence of the occurrence and the latitude on the solar activity based on kilometric continuum observed by INTERBALL-1, the latitude dependence is examined for GEOTAIL observations in quiet time in 1996 ([**Hashimoto et al.**, 1999]) and in active time from July, 2000 to June, 2001, the dashed and the solid lines in Figures 7, respectively. Although the occurrence of the latter is a little higher, no clear latitude dependency is confirmed. No dip of the occurrence near the equator is not found in the 2000-2001 data.

It is confirmed that kilometric continuum is generated at steep density gradients at density irregularities in the equatorial region. These irregularities exist not only at the plasmapause, but also inside the plasmapause and in notches. Although the observations are consistent with the mode conversion at the plasma frequency, CRRES observations and simultaneous observations by GEOTAIL and IMAGE have shown evidences not consistent with the beaming theory [Jones, 1980 and 1981]. This is the first clear evidence of a broad-band emission cone. Especially, IMAGE observed kilometric continuum up to about 30° in north and south latitudes.

The beaming theory shows a good conversion rate at a beaming angle. Jones [1988] indicated more precise conversion rate using the full-wave theory. There are, however, no conversion near the equator. On the other hand, the CRRES and IMAGE satellites observed kilometric continuum in wide latitudes including the equator. The beaming theory is not consistent with the present observations since the generation is expected to occur in wide angles including the equator. The theory itself is just an application of Snell's law. The conversion of Z mode waves to O mode waves is basically expected to follow this theory. Since our observations, however, indicated clear objections, new explanation on the propagation of continuum is expected.

The simultaneous observations could also be the highest frequency continuum enhancement so far observed since they are associated with a high energy electron injection event observed at 20-21 UT.

Acknowledgment.

We thank H. Oya for his useful comments.

References

Anderson, R. R., D. A. Gurnett, and D. L. Odem, CRRES Plasma Wave Experiment, J. Spacecraft Rockets, 29, 570–573, 1992.

Carpenter, D. L., and R. R. Anderson, An ISEE/whistler model of equatorial electron density in the magnetosphere, J. Geophys. Res., 97, 1097–1108, 1992.

Carpenter, D. L., R. R. Anderson, W. Calvert, M. B. Moldwin, CRRES observations of density cavities inside the plasmasphere, J. Geophys. Res., 105, 23,323–23,338, 2000.

Gough, M. P., Nonthermal continuum emissions associated with electron injections: Remote plasmapause sounding, Planet. Space Sci., 30, 657, 1982.

Green, J. L., B. R. Sandel, S. F. Fung, D. L. Gallagher, and B. W. Reinisch, On the Origin of Kilometric Continuum, J. Geophys. Res., 107, 10.1029/2001JA000193, 2002.

Green, J. L., Boardsen, S., Fung, S. F., Matsumoto, H., Hashimoto, K., Anderson, R. R., Sandel, B. R., Reinisch, B. W., Association of kilometric continuum radiation with plasmaspheric structures, J. Geophys. Res., 109, A03203, 10.1029/2003JA010093, 2004.

Hashimoto, K., W. Calvert, and H. Matsumoto, Kilometric continuum detected by Geotail, J. Geophys. Res., 104, 28645-28656, 1999.

Jones, D., Source of terrestrial nonthermal radiation, Nature, 260, 686–689, 1976.

Jones, D., Latitudinal beaming of planetary radio emissions, Nature, 288, 225–229, 1980.

Jones, D., Beaming of terrestrial myriametric radiation, Adv. Space Res., 1, 373–376, 1981.

Jones, D., Terrestrial myriametric radiation from the Earth's plasmapause, Planet. Space Sci., 30, 399–410, 1982.

Jones, D., W. Calvert, D. A. Gurnett, and R. L. Huff, Observed beaming of terrestrial myriametric radiation, Nature, 328, 391–395, 1987.

Jones, D., Planetary radio emissions from low magnetic latitudes - Observations and theories, in Planetary Radio Emissions II, 245–281, 1988

Kasaba, Y., H. Matsumoto, K. Hashimoto, R. R. Anderson, J.-L. Bougeret, M. L. Kaiser, X. Y. Wu, and I. Nagano, Remote sensing of the plasmapause during substorms: GEOTAIL observation of nonthermal continuum enhancement, J. Geophys. Res., 103, 20389–20405, 1998.

Kurth, W. S., D. A. Gurnett, and R. R. Anderson, Escaping nonthermal continuum radiation, J. Geophys. Res., 86, 5519–5531, 1981.

Kuril'chik, V. N., I. F. Kopaeva, and S. V. Mironov, INTERBALL-1 Observations of the Kilometric "Continuum" of the Earth's Magnetosphere, Cosmic Research, 42, 1–7, 2004.

Matsumoto, H., I. Nagano, R. R. Anderson, H. Kojima, K. Hashimoto, M. Tsutsui, T. Okada, I. Kimura, Y. Omura, and M. Okada, Plasma wave observations with GEOTAIL spacecraft, J. Geomagn. Geoelectr., 46, 59–95, 1994.

Menietti, J. D. , R. R. Anderson, J. S. Pickett, and D. A. Gurnett, and H. MatsumotoNear-source and remote observations of kilometric continuum radiation from multi-spacecraft observations, J. Geophys. Res., 108, 1393, doi:10.1029/2003JA009826, 2003

Morgan, D. D., and D. A. Gurnett, The source location and beaming of terrestrial continuum radiation, J. Geophys. Res., 96, 9595–9613, 1991.

Reinisch, B. W., D. M. Haines, K. Bibl, G. Cheney, I. A. Galkin, X. Huang, S. H. Myers, G. S. Sales, R. F. Benson, S. F. Fung, J. L. Green, S. Boardsen, W. W. L. Taylor, J.-L. Bougeret, R. Manning, N. Meyer-Vernet, M. Moncuquet, D. L. Carpenter, D. L. Gallagher P. Reiff, The Radio Plasma Imager investigation on the IMAGE spacecraft, Space Sci. Rev., 91, 319, 2000.

Sandel, B. R., R. A. King, W. A. King, W. T. Forrester, D. L. Gallagher, A. L. Broadfoot, and C. C. Curtis, Initial results from the IMAGE Extreme Ultraviolet Imager, Geophys. Res. Letts., 28, 1439–1442, 2001.

R. R. Anderson, The University of Iowa, Department of Physics and Astronomy, IA 52242-1479

J. L. Green, Code 630, NASA/GSFC, Greenbelt, MD 20771

K. Hashimoto and H. Matsumoto, Research Institute for Sustainable Humanosphere, Kyoto University, Uji, Kyoto 611-0011, Japan. (e-mail: kozo@rish.kyoto-u.ac.jp)

Received _____

Submitted to J. Geophys. Res., August 9, 2004

Figure Captions

Figure 1. CRRES observations on October 10, 1990.

Figure 2. CRRES observations on September 6, 1990.

Figure 3. CRRES observations on August 19, 1990.

Figure 4. Calculation of beaming angles for the August 19 observations.

Figure 5. IMAGE and GEOTAIL observations and their orbits on May 29–30, 2003

Figure 6. Latitude dependence of the occurrence in 1996 and 2000-1

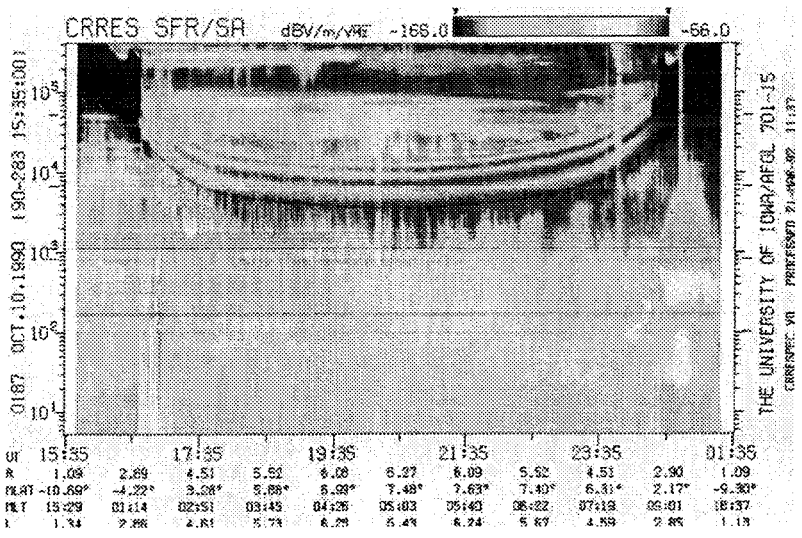

Figure 1. CRRES observations on October 10, 1990.

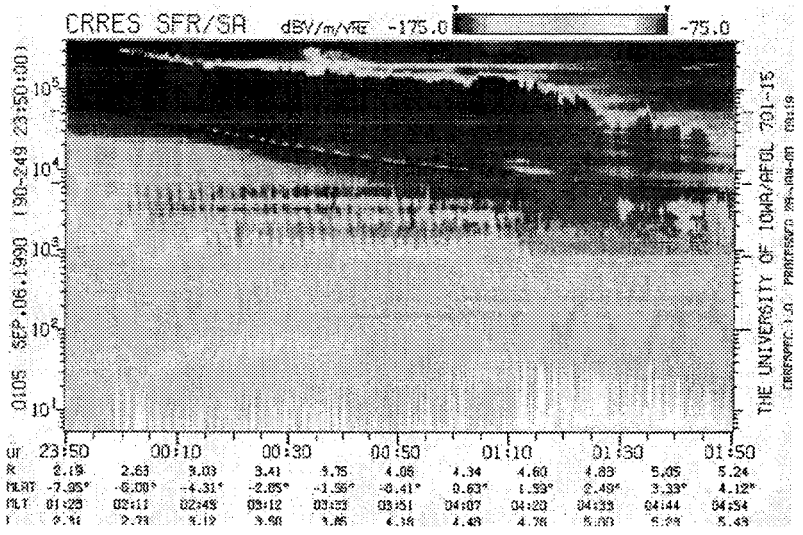

Figure 2. CRRES observations on September 6, 1990.

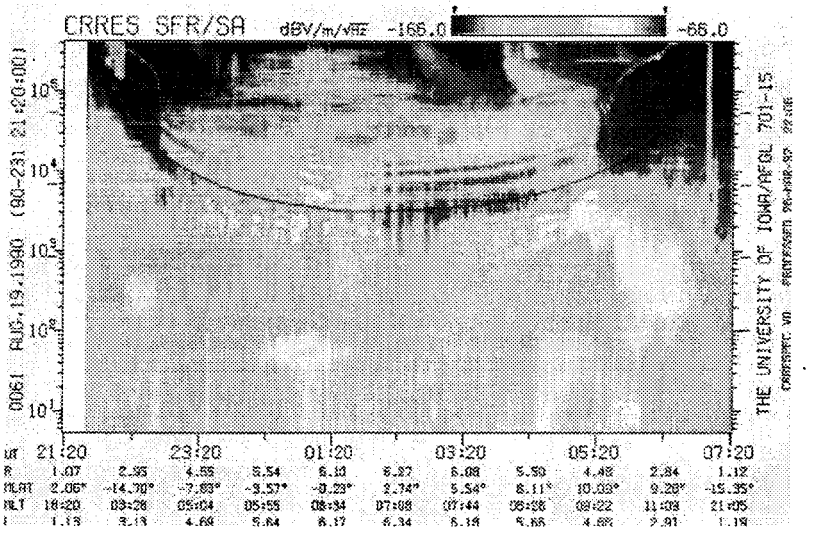

Figure 3. CRRES observations on August 19, 1990.

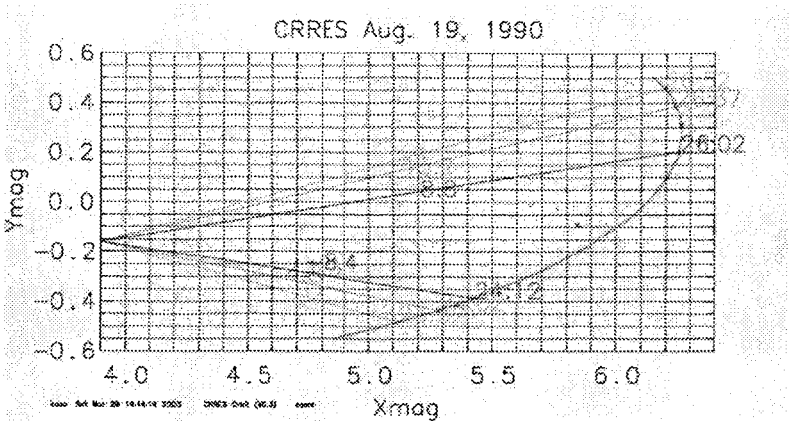

Figure 4. Calculation of beaming angles for the August 19 observations.

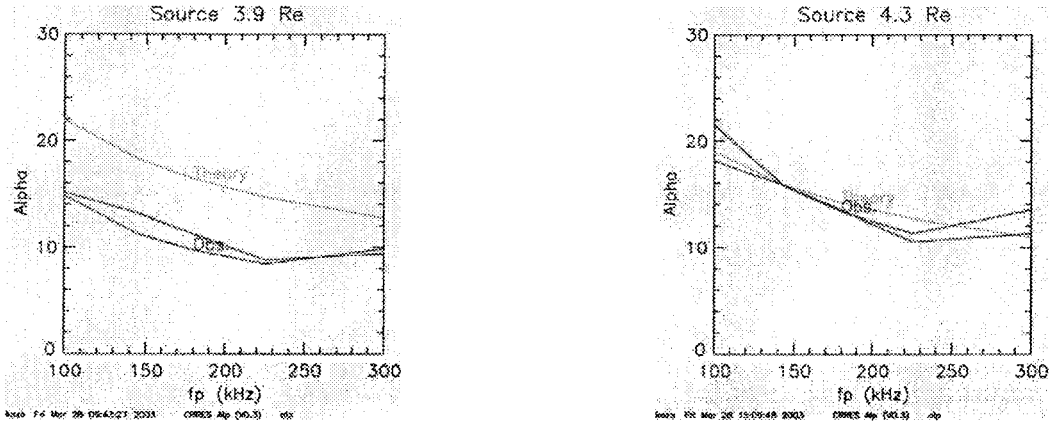

Figure 5. a and b. Comparison between the calculations and the theory.

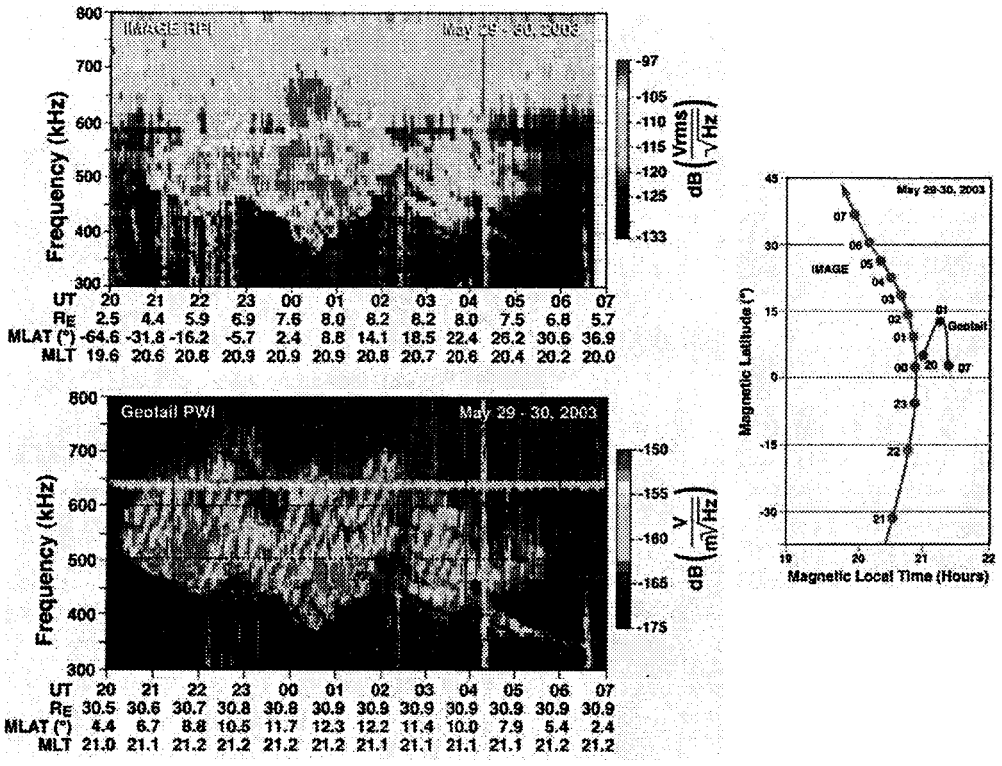

Figure 6. IMAGE and GEOTAIL observations and their orbits on May 29–30, 2003

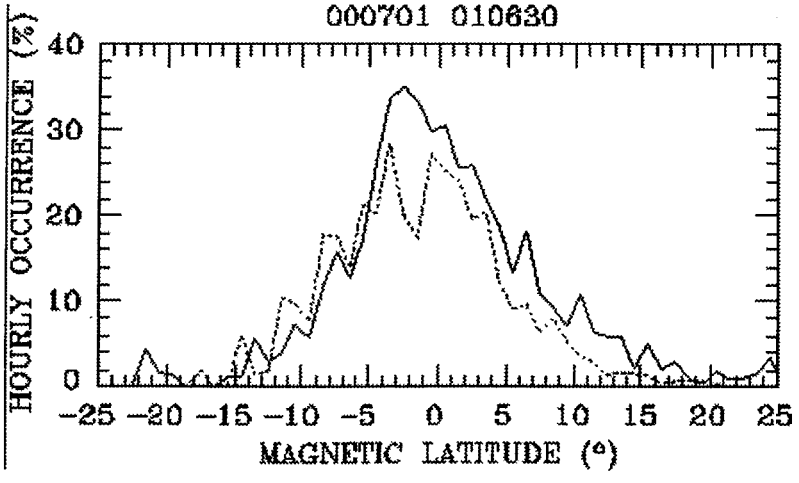

Figure 7. Latitude dependence of the occurrence in 1996 and 2000-1